

Front propagation of a sexual population with evolution of dispersion: a formal analysis *

Léonard Dekens[†]Florian Lavigne[‡]

January 1, 2022

Abstract

The adaptation of biological species to their environment depends on their traits. When various biological processes occur (survival, reproduction, migration, *etc.*), the trait distribution may change with respect to time and space. In the context of invasions, when considering the evolution of a heritable trait that encodes the dispersive ability of individuals, the trait distribution develops a particular spatial structure that leads to the acceleration of the front propagation. That phenomenon is known as spatial sorting. Many biological examples can be cited like the bush cricket in Britain, the cane toad invasion in Australia or the common myna one in South Africa.

Adopting this framework, recent mathematical studies have led to highlight the influence of the reproductive mode on the front propagation. Asexual populations have been shown to spread with an asymptotic rate of $t^{3/2}$ in a minimal reaction-diffusion model, whereas the analogous rate for sexual populations is of $t^{5/4}$ (where t denotes the time). However, the precise description of the behaviour of the front propagation in the sexual case is still an open question.

The aim of this paper is to give precise approximations for large times of its position, as well as some features of the local trait distribution at the front. To do so, we solve explicitly the asymptotic problem derived formally. Numerical simulations are shown to confirm these calculations.

Keywords: Partial Differential Equation, Wave Front, Invasion, Sexual Reproduction, Evolution of Dispersion, Spatial Sorting.

AMS: 35Q92, 92D15, 92D25, 35R09, 35B40, 35K57.

*European Research Council (ERC) under the European Union's Horizon 2020 research and innovation program (grant agreement No 639638) and the ANR projects NONLOCAL (ANR-14-CE25-0013) and RESISTE (ANR-18-CE45-0019).

[†]Institut Camille Jordan, UMR5208 UCBL/CNRS, Université de Lyon; INRIA, Dracula Team. (dekins@math.univ-lyon1.fr).

[‡]Aix Marseille Univ, CNRS, Centrale Marseille, I2M, Marseille, France (florian.lavigne@univ-amu.fr, florian.lavigne@inra.fr).

1 Introduction

Individuals can be more or less adapted to their environment, depending on their traits. Various processes shape the trait distributions: some of them intervene locally, like survival and reproduction, and others highly depend on the spatial structure of the environment, like migration. Biological invasions are an example of a process where the role of space is structuring. As the combination of locally limited amount of resources and large available inhabited space tends to drive individuals further away, the ability to explore can be selected upon. Morphological features can therefore evolve to increase dispersion: closer to the front of the invasion, cane toads in Australia tends to develop longer legs B. Phillips et al. 2006, common myna birds in South Africa and *conocephalus discolor* bush cricket in Britain, larger wings Berthouly-Salazar et al. 2012; Thomas et al. 2001.

However, that process is not homogeneous in space: individuals with higher dispersal ability are typically located at the range expansion front. This phenomenon is called *spatial sorting*. Its relationship with the evolution of dispersion has been studied by biologists for the past two decades Birzu, Hallatschek, and Korolev 2017; Shine, Brown, and B. L. Phillips 2011; Thomas et al. 2001; Travis and Dytham 2002; Travis, Mustin, et al. 2009. More recently, mathematical studies have been quantifying its influence on the asymptotic speed of the invasion. Our model equation describes the effects of evolution of a trait $\theta > 1$, which determines the dispersion rate, in space ($\mathbf{x} \in \mathbb{R}$) and through time ($t \geq 0$) in a population subject to sexual reproduction and competition. The trait density $f(t, \mathbf{x}, \theta)$ evolves according to:

$$\partial_t f(t, \mathbf{x}, \theta) = r \underbrace{[B[f](t, \mathbf{x}, \theta)]}_{\text{reproduction}} - \underbrace{K^{-1} \varrho(t, \mathbf{x}) f(t, \mathbf{x}, \theta)}_{\text{competition}} + \underbrace{\theta \Delta_{\mathbf{x}} f(t, \mathbf{x}, \theta)}_{\text{dispersion}}, \quad (1)$$

for $\Delta_{\mathbf{x}}$ the Laplace operator with respect to \mathbf{x} .

When the dispersal rate is possibly unbounded, the relationship between the front propagation and sustained spatial sorting leads to an acceleration of front propagation N. Berestycki, Mouhot, and Raoul 2015; Bouin, Calvez, et al. 2012; Bouin, Henderson, and Ryzhik 2017; Calvez, Henderson, et al. 2018, contrary to the case of constant dispersion for which it is well established that the front expands asymptotically at constant speed Aronson and Weinberger 1978; H. Berestycki, Hamel, and Nadin 2008; Fang and Zhao 2011; Genieys, Volpert, and Auger 2006; Gourley 2000; Hamel and Ryzhik 2014; Mirrahimi and Raoul 2013.

To our knowledge, analytical results describing the asymptotic accelerating rate of propagation exist only for asexual (clonal) populations (*e.g.*, see N. Berestycki, Mouhot, and Raoul 2015; Bouin, Henderson, and Ryzhik 2017; Calvez, Henderson, et al. 2018), for which the reproduction operator in (1) is :

$$B[f] = f + \sigma^2 \Delta_{\theta} f,$$

for some constant $\sigma^2 \geq 0$ depending on the mutation variance and mutation rate and for Δ_{θ} the Laplace operator with respect to θ . In this case, the position of the population

range asymptotically expands as $t^{3/2}$ (see N. Berestycki, Mouhot, and Raoul 2015; Bouin, Calvez, et al. 2012; Bouin, Henderson, and Ryzhik 2017; Calvez, Henderson, et al. 2018 for more details). Furthermore, the precise asymptotic position of the front has been derived in Calvez, Henderson, et al. 2018, by specifying the prefactor term. The value of this prefactor is sensitive to how the competition is modelled : when it is local in trait, it has been shown to be equal to a larger value N. Berestycki, Mouhot, and Raoul 2015; Bouin, Calvez, et al. 2012; Bouin, Henderson, and Ryzhik 2017.

However, as reproductive mode is thought to potentially significantly influence the rate of propagation Williams, Hufbauer, and Miller 2019, we take interest into invasions of sexually reproducing populations. An analogous model as for asexual populations can be built using Fisher’s infinitesimal model, a model of allelic segregation that has been studied and used for a century in quantitative genetics, a branch of evolutionary biology Barton, Etheridge, and Véber 2017; Bulmer 1972; Fisher 1919; Lange 1978; Tufto 2000; Turelli 2017; Turelli and Barton 1994. This model has also been used to model sexually reproducing populations in several integro-differential studies Bouin, Bourgeron, et al. 2018; Calvez, Garnier, and Patout 2019; Mirrahimi and Raoul 2013; Raoul 2017, with the following reproduction operator in (1):

$$B[f](t, x, \theta) = \iint_{(\theta_{\min}, \infty)^2} \mathcal{G}_\lambda \left[\theta - \frac{\theta_1 + \theta_2}{2} \right] \frac{f(t, x, \theta_1) f(t, x, \theta_2)}{\varrho(t, x)} d\theta_1 d\theta_2.$$

It assumes that the trait of the offspring is given by the mean parental trait up to a random normal deviation given by \mathcal{G}_λ with constant segregational variance λ^2 . Using this model, the authors of the report Calvez, Crevat, et al. 2019 predicted and numerically confirmed an asymptotic invasion rate of $t^{5/4}$ for sexually reproducing populations.

However, to understand the complexity of the interplay between ecology and evolution in the dynamics of an invasion, the relationship between the propagation and the trait distribution has to be untangled. That requires to describe precisely the trait distribution and the effect of spatial sorting at the front of the invasion, which is the goal of this paper. First, we present our model and the explicit formula that we derive to approximate the position of the front propagation and its local trait distribution at large times (Section 2). Next, we present numerical simulations that confirm this formula (Section 3). Finally, we derive formally the limit problem for large times and find an explicit solution to it (Section 4).

2 Deterministic model

In this section, we present the integro - differential model that we use and state our formal result as an approximation of the solutions of the resulting equation. The population is described according to its location $x \in \mathbb{R}$ and its dispersive trait $\theta \in (\theta_{\min}, +\infty)$, with $\theta_{\min} > 0$. Here we are interested by the evolution of the density $f(t, x, \theta)$ of individuals being at time $t \geq 0$ at the location $x \in \mathbb{R}$, presenting the trait θ . We also assume that, initially, the density is compactly supported.

Our model. The evolution of the density $\mathbf{f}(\mathbf{t}, \mathbf{x}, \boldsymbol{\theta})$ can be modeled with the following reaction - diffusion equation for all $\mathbf{t} > 0$, $\mathbf{x} \in \mathbb{R}$ and $\boldsymbol{\theta} > \boldsymbol{\theta}_{\min}$:

$$\partial_t \mathbf{f}(\mathbf{t}, \mathbf{x}, \boldsymbol{\theta}) = \mathbf{r} \left[\mathbf{B}[\mathbf{f}](\mathbf{t}, \mathbf{x}, \boldsymbol{\theta}) - \mathbf{K}^{-1} \boldsymbol{\varrho}(\mathbf{t}, \mathbf{x}) \mathbf{f}(\mathbf{t}, \mathbf{x}, \boldsymbol{\theta}) \right] + \boldsymbol{\theta} \Delta_{\mathbf{x}} \mathbf{f}(\mathbf{t}, \mathbf{x}, \boldsymbol{\theta}), \quad (2)$$

where $\mathbf{r} > 0$ and $\mathbf{K} > 0$ are fixed constants, and $\boldsymbol{\varrho}(\mathbf{t}, \mathbf{x}) := \int_{\boldsymbol{\theta}_{\min}}^{\infty} \mathbf{f}(\mathbf{t}, \mathbf{x}, \boldsymbol{\theta}) d\boldsymbol{\theta}$ is the population size at $\mathbf{x} \in \mathbb{R}$ and time $\mathbf{t} > 0$. We will detail the reaction term $\mathbf{B}[\mathbf{f}]$ later. At first, let us discuss the modelling motivation of each term.

First, the term $\mathbf{r} \left[\mathbf{B}[\mathbf{f}](\mathbf{t}, \mathbf{x}, \boldsymbol{\theta}) - \mathbf{K}^{-1} \boldsymbol{\varrho}(\mathbf{t}, \mathbf{x}) \mathbf{f}(\mathbf{t}, \mathbf{x}, \boldsymbol{\theta}) \right]$ is analogous to a logistic growth term that models *reproduction* and *competition*. More precisely, the reproduction term $\mathbf{B}[\mathbf{f}](\mathbf{t}, \mathbf{x}, \boldsymbol{\theta})$ represents the number of new individuals that are born with the trait $\boldsymbol{\theta}$ at time $\mathbf{t} \geq 0$ and position $\mathbf{x} \in \mathbb{R}$ and we will detail the modelling of the segregational process later. Moreover, at point $\mathbf{x} \in \mathbb{R}$ and at time $\mathbf{t} \geq 0$, there is a competition between individuals for resources, related to the parameter \mathbf{K} which is a measure of the *carrying capacity* of the environment. When the local population size at \mathbf{x} is relatively small - $\boldsymbol{\varrho}(\mathbf{t}, \mathbf{x}) \ll \mathbf{K}$ - the local population disposes of enough resources to allow an exponential - like growth, while, if $\boldsymbol{\varrho}(\mathbf{t}, \mathbf{x}) \gg \mathbf{K}$, then competition between individuals is strong, and consequently the local population size decreases. The constant $\mathbf{r} > 0$ is therefore called *growth rate at low density*.

Then, the diffusion term $\boldsymbol{\theta} \Delta_{\mathbf{x}} \mathbf{f}$ models the *dispersion* phenomenon. Individuals are assumed to diffuse through space at each time \mathbf{t} , at a rate given by the dispersive trait $\boldsymbol{\theta} \geq \boldsymbol{\theta}_{\min}$. When $\boldsymbol{\theta}$ gets larger, it models situations like having longer legs or bigger wings, which potentially give an advantage to explore a new environment faster.

Finally, let us come back to the reproduction operator $\mathbf{B}[\mathbf{f}]$. We consider a monoeccious population in which the individuals breed randomly and only with those at the same location $\mathbf{x} \in \mathbb{R}$. At time \mathbf{t} , an individual with trait $\boldsymbol{\theta}_1$ finds a mate with trait $\boldsymbol{\theta}_2$ with the probability density equal to the trait frequency at position \mathbf{x} : $\mathbf{f}(\mathbf{t}, \mathbf{x}, \boldsymbol{\theta}_2) / \boldsymbol{\varrho}(\mathbf{t}, \mathbf{x})$. To model the segregation, we use Fisher's infinitesimal model, which classically states that the offspring trait differs from the mean parental trait $(\boldsymbol{\theta}_1 + \boldsymbol{\theta}_2) / 2$ according to a normal distribution with a segregational variance $\boldsymbol{\lambda}^2 > 0$ assumed to be constant and independent of the parental trait values. These assumptions imply the following formulation of the reproduction term:

$$\mathbf{B}[\mathbf{f}](\mathbf{t}, \mathbf{x}, \boldsymbol{\theta}) = \iint_{(\boldsymbol{\theta}_{\min}, \infty)^2} \mathcal{G}_{\boldsymbol{\lambda}} \left[\boldsymbol{\theta} - \frac{\boldsymbol{\theta}_1 + \boldsymbol{\theta}_2}{2} \right] \frac{\mathbf{f}(\mathbf{t}, \mathbf{x}, \boldsymbol{\theta}_1) \mathbf{f}(\mathbf{t}, \mathbf{x}, \boldsymbol{\theta}_2)}{\boldsymbol{\varrho}(\mathbf{t}, \mathbf{x})} d\boldsymbol{\theta}_1 d\boldsymbol{\theta}_2.$$

The term $\mathcal{G}_{\boldsymbol{\lambda}}[\boldsymbol{\theta} - (\boldsymbol{\theta}_1 + \boldsymbol{\theta}_2) / 2]$, symbolizing the stochasticity of the segregation process, is defined as a normalized Gaussian density with variance $\boldsymbol{\lambda}^2 > 0$, that is:

$$\mathcal{G}_{\boldsymbol{\lambda}}(\boldsymbol{\theta}) := \frac{1}{\sqrt{2\pi\boldsymbol{\lambda}^2}} \exp \left[-\frac{\boldsymbol{\theta}^2}{2\boldsymbol{\lambda}^2} \right]. \quad (3)$$

Let us rescale the equation by setting :

$$t = \mathbf{r} \mathbf{t}, \quad x = \sqrt{\frac{\mathbf{r}}{\boldsymbol{\theta}_{\min}}} \mathbf{x}, \quad \theta = \frac{\boldsymbol{\theta}}{\boldsymbol{\theta}_{\min}}, \quad \text{and} \quad f(t, x, \theta) = \frac{\boldsymbol{\theta}_{\min}}{\mathbf{K}} \mathbf{f}(\mathbf{t}, \mathbf{x}, \boldsymbol{\theta}).$$

Then, we can simplify the previous PDE into:

$$\partial_t f(t, x, \theta) = B[f](t, x, \theta) - \varrho(t, x) f(t, x, \theta) + \theta \Delta_x f(t, x, \theta), \quad (4)$$

with the rescaled population size:

$$\varrho(t, x) = \int_1^\infty f(t, x, \theta) d\theta.$$

By this simplification, the reproduction term is:

$$B[f](t, x, \theta) = \iint_{(1, \infty)^2} \mathcal{G}_\lambda \left[\theta - \frac{\theta_1 + \theta_2}{2} \right] f(t, x, \theta_1) \frac{f(t, x, \theta_2)}{\varrho(t, x)} d\theta_1 d\theta_2, \quad (5)$$

where \mathcal{G}_λ is given by (3), and $\lambda = \lambda/\theta_{\min}$. One can notice the truncation at the bottom level $\theta_{\min} = 1$, chosen for the sake of simplicity (note that θ_{\min} can only take positive values), which does not influence the long time asymptotics in the subsequent analysis as θ is expected to take large values at the front.

Main result. In this paper, we denote by $x \cdot J$, for some $x \in \mathbb{R}$ and $J = [a, b]$, the interval $[xa, xb]$ and $|J|$ the length of the interval J . As some computations are only formal, we state our main result as a conjecture:

Conjecture 1. *Define the constant*

$$y_c = 4 \left(\frac{\lambda}{3} \right)^{1/2}. \quad (6)$$

There exists an interval of trait values J_0 centered in 1 such that, for all $J \subset J_0$ open interval centered in 1, the density f at large time $t \geq 0$ can be approximated by:

$$f(t, x, \theta) = \begin{cases} \exp \left[-\frac{1}{4\lambda^2} [\theta - \lambda^{4/5}(6x^2)^{1/5}]^2 + \mathcal{O}_{t \rightarrow \infty}(|J|^2) \right], \\ \text{for } x \leq y_c t^{5/4}, \theta \in \lambda^{4/5}(6x^2)^{1/5} \cdot J, \\ \exp \left[\left(1 - \left(\frac{x}{y_c t^{5/4}} \right)^{4/3} \right) t \right] \exp \left[-\frac{1}{4\lambda^2} \left[\theta - \left(\frac{3\lambda^2 x^2}{2t} \right)^{1/3} \right]^2 + \mathcal{O}_{t \rightarrow \infty} \left(|J|^2 \frac{x^{8/3}}{t^{10/3}} \right) \right], \\ \text{for } x \geq y_c t^{5/4}, \theta \in \left(\frac{3\lambda^2 x^2}{2t} \right)^{1/3} \cdot J. \end{cases}$$

For $x \geq y_c t^{5/4}$, we call the coefficient $\exp \left[\left(1 - \left(\frac{x}{y_c t^{5/4}} \right)^{4/3} \right) t \right]$ the prefactor of the trait distribution, which is of the form $\exp \left[-c \left(\frac{x}{y_c t^{5/4}} \right) t \right]$, where the function c is positive and increasing on $]1, +\infty[$.

The justification of this conjecture is postponed to Section 4.

Conjecture 1 yields that at each time $t \geq 0$ large enough, the propagating front is at the position:

$$X(t) \approx y_c t^{5/4} = 4 \left(\frac{\lambda}{3} \right)^{1/2} t^{5/4}. \quad (7)$$

Additionally, at large time t and all space position $x \in \mathbb{R}$, the dispersive trait is normally distributed, with variance $2\lambda^2$. Behind the front, *i.e.*, at all position $x \ll X(t)$, the mean of the dispersive trait $\bar{\theta}$ can be approximated by the value:

$$\bar{\theta}(x) \approx \lambda^{4/5} (6x^2)^{1/5}, \quad (8)$$

while ahead of the front, *i.e.*, at all position $x \gg X(t)$, it can be approximated by:

$$\bar{\theta}(t, x) \approx \left(\frac{3\lambda^2 x^2}{2t} \right)^{1/3}. \quad (9)$$

Moreover, the prefactor of the distribution trait, $\exp \left[-c \left(\frac{y}{y_c} \right) t \right]$, with $c > 0$ increasing on $]1, +\infty[$ and $y = t^{-5/4}x$, indicates that, ahead of the front, the population size presumably decreases with regard to the rescaled space variable y at a given time $t > 0$.

3 Simulations and validation

In this section, we display numerical simulations, in order to validate the approximation of the solution of the Eq. (4) provided by Conjecture 1. The initial distribution used for simulation is assumed to be a truncated Gaussian distribution:

$$f(0, x, \theta) = \sqrt{\frac{2}{\pi}} \exp \left[-\frac{x^2 + (1 - \theta)^2}{2} \right] \mathbb{1}_{\theta \geq 1}, \quad (10)$$

with $\mathbb{1}_{\theta \geq 1}$ the characteristic function of $\{\theta \geq 1\}$. The segregational variance λ^2 is taken equal to $1/2$. The discretization of the sexual reproduction term $B[f]$ represents the biggest challenge for the simulations, in comparison to the asexual case (see Calvez, Crevat, et al. 2019).

3.1 Scheme

We consider $x_{\max} \geq 0$ and $\theta_{\max} \geq 1$ so that we work with tuples (x, θ) in the bounded domain $[0, x_{\max}] \times [1, \theta_{\max}]$, discretized with the meshes $(x_i)_{1 \leq i \leq N_x}$ and $(\theta_j)_{1 \leq j \leq N_\theta}$, respectively of step length $\delta x > 0$ and $\delta \theta > 0$. As for the time discretization, let $\delta t > 0$ be a time step length, and let us define for all $n \in \mathbb{N}$, $t_n := n \delta t$. We denote by A_x^N the matrix of the discrete Laplace operator in x of size N_x with Neumann boundary condition at $x = 0$ and Dirichlet boundary condition at $x = x_{\max}$:

$$A_x^N = \frac{1}{\delta x^2} \begin{pmatrix} -1 & 1 & & & (0) \\ 1 & -2 & 1 & & \\ & \ddots & \ddots & \ddots & \\ & & 1 & -2 & 1 \\ (0) & & & 1 & -2 \end{pmatrix} \in \mathcal{M}_{N_x}(\mathbb{R}),$$

and the diagonal matrix:

$$D_\theta = \begin{pmatrix} \theta_1 & & (0) \\ & \ddots & \\ (0) & & \theta_{N_\theta} \end{pmatrix} \in \mathcal{M}_{N_\theta}(\mathbb{R}).$$

Futhermore, we introduce a 3D hypermatrix $G_\theta \in M_{N_\theta, N_\theta, N_\theta}(\mathbb{R})$ such that:

$$\forall i, j, k, G_\theta(i, j, k) = \mathcal{G}_\lambda \left[\theta_k - \frac{\theta_i + \theta_j}{2} \right],$$

representing the discretization of the segregation kernel (\mathcal{G}_λ given by (3)).

For all $n \in \mathbb{N}$, we approximate $(f(t_n, x_i, \theta_j))_{1 \leq i \leq N_x, 1 \leq j \leq N_\theta}$ by a matrix:

$$F^n = \left(F_{ij}^n \right)_{1 \leq i \leq N_x, 1 \leq j \leq N_\theta} \in \mathcal{M}_{N_x, N_\theta}(\mathbb{R}),$$

and the population size $(\varrho(t_n, x_i))_{1 \leq i \leq N_x}$ by the vector:

$$\tilde{\varrho}_i^n := \sum_{k=1}^{N_\theta} F_{i,k}^n \delta\theta \approx \varrho(t_n, x_i),$$

using the following scheme. At each time iteration n ,

1. For every index $1 \leq k \leq N_\theta$, we compute the vector $V_{k,l}^n$ defined by:

$$\forall l, V_{k,l}^n := \delta\theta^2 \left[F^n G_\theta(\cdot, \cdot, k) (F^n)^T \right]_{ll}.$$

We can check that $V_{k,l}^n$ is the discretization of the reproduction integral term:

$$\begin{aligned} V_{k,l}^n &= \delta\theta^2 \sum_{i,j=1}^{N_\theta} F_{l,i}^n G_\theta(i, j, k) F_{l,j}^n, \\ &\approx \delta\theta^2 \sum_{i,j=1}^{N_\theta} f(t_n, x_l, \theta_i) \mathcal{G}_\lambda \left[\theta_k - \frac{\theta_i + \theta_j}{2} \right] f(t_n, x_l, \theta_j), \\ &\approx \iint_{(1,\infty)^2} f(t_n, x_l, \theta_1) \mathcal{G}_\lambda \left[\theta_k - \frac{\theta_1 + \theta_2}{2} \right] f(t_n, x_l, \theta_2) d\theta_1 d\theta_2. \end{aligned}$$

Now to compute the reproduction matrix $\text{Mat}_{\text{Reprod}} \in \mathcal{M}_{N_x, N_\theta}(\mathbb{R})$, we need to divide the previous quantities by the corresponding $\tilde{\varrho}_i^n$. To be consistent, we set:

$$\forall i, k, \text{Mat}_{\text{Reprod}}^n(i, k) = \begin{cases} V_{k,i}^n / \tilde{\varrho}_i^n, & \text{if } \tilde{\varrho}_i^n > 0, \\ 0, & \text{else.} \end{cases}$$

2. We define the diagonal matrix $D_\varrho^n := \text{diag}((\tilde{\varrho}_i^n)_{1 \leq i \leq N_x}) \in \mathcal{M}_{N_x}(\mathbb{R})$.

3. We approximate in time using an explicit Euler scheme that is for all $n \in \mathbb{N}$:

$$F^{n+1} := F^n + \delta t \left[A_x^N \times F^n \times D_\theta + r \left(\text{Mat}_{\text{Reprod}}^n - K^{-1} \times D_\theta^n \times F^n \right) \right]. \quad (11)$$

In this section, the parameters r and K are equal to 1. The general scheme 11 is used in supplementary materials, to show the effects of different parameters on the invasion.

To be sure that this scheme gives a good approximation of the solution of the PDE (4), the spatial step δx is taken large enough.

3.2 Numerical results

We show our results of simulations of the solution of the Eq. (4) in two figures Fig. 1 and Fig. 2. In the first one, we display different features of the front, whereas in the second one, we compare the numerical trait distribution behind the front with the approximation formally obtained in Conjecture 1.

In the top subfigure Fig. 1 (a), the population size $\varrho(t, x)$ is displayed at multiple time regularly spaced between $t = 20$ and $t = 200$ for different scaled position x . As expected, thanks to Fig. 1 (a), we can see that this front accelerates: there exists a constant y_c^{num} such that the front at time t is at position:

$$X^{num}(t) = y_c^{num} t^{5/4},$$

where the numerical front position $X^{num}(t)$ at time $t \geq 0$ is defined by:

$$X^{num}(t_n) = x_{i^{num}(t_n)}, \quad \text{with} \quad i^{num}(t_n) := \underset{1 \leq i \leq N_x}{\text{argmin}} |\tilde{\varrho}_i^n - 0.01|. \quad (12)$$

More precisely, thanks to a linear regression, the constant y_c^{num} can be approximated by 2.1, and the exponent of t by 1.22 (with $R^2 = 1$ and $p\text{-value} < 10^{-4}$). These numerical results are consistent with (7), which numerically gives:

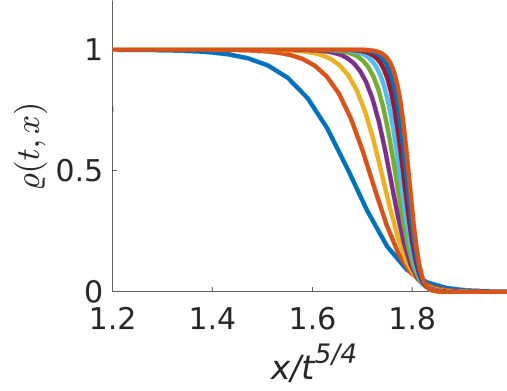
$$X(t) = 4 \left(\frac{1}{2 \times 9} \right)^{1/4} t^{5/4} \approx 1.94 t^{5/4}.$$

With Fig. 1 (b), we confirm that the mean of the dispersive trait at the front that we get from the numerical simulations is quite consistent with the approximation given by Conjecture 1. Precisely, let us define the mean of the dispersive trait $\bar{\theta}^{num}(t)$ at the front position $X^{num}(t)$, given by:

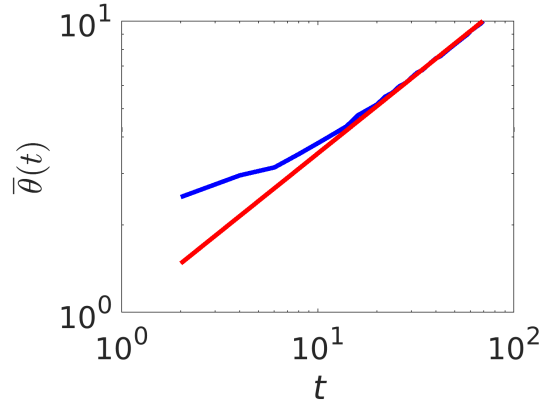
$$\bar{\theta}^{num}(t) := \frac{\int_{\mathbb{R}} \theta f(t, X^{num}(t), \theta) d\theta}{\varrho(t, X^{num}(t))}. \quad (13)$$

Using a linear regression on the values for $t \in [60, 200]$ (illustrated in Fig. 1 (b)), the mean of the dispersive trait $\bar{\theta}^{num}$ can be approximated by:

$$\bar{\theta}^{num}(t) \approx 1.02 t^{0.54}, \quad (R^2 = 1, p\text{-value} < 10^{-14}).$$



(a)



(b)

Figure 1: **Simulations of the invasion of a sexual population**, associated to the Eq.(4) with parameters $\delta t = 0.02$, $\delta x = 4$, $\delta\theta = 2/3$, $x_{\max} = 3000$ and $\theta_{\max} = 201$. (a) Plot of the population size $\varrho(t, \cdot)$ for successive fixed times at regular intervals from $t = 20$ to $t = 200$, with respect to the auto - similar variable $xt^{-5/4}$. (b) Plot of the mean of the dispersive trait $\bar{\theta}^{num}(t)$ (see (13)) at the front position with respect to time (blue curve) and of the function $t \rightarrow 1.02t^{0.54}$ (red curve), in log - log scale.

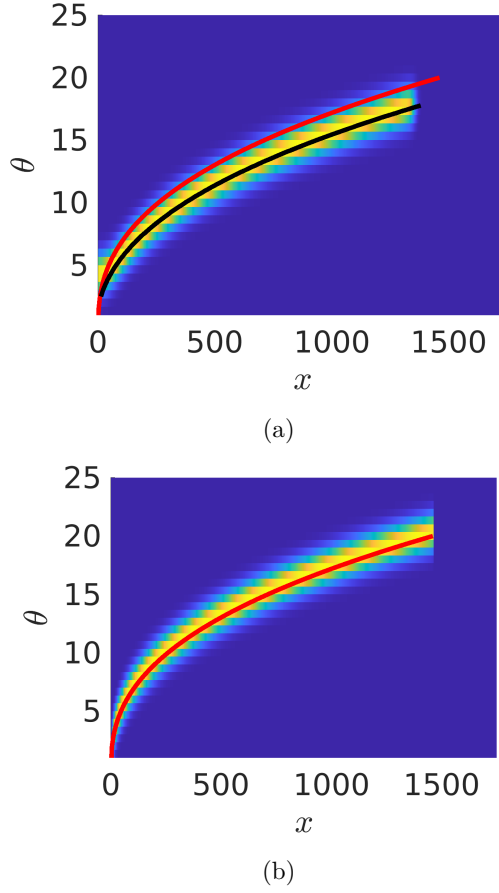


Figure 2: **Contour lines of the trait distribution of a sexual population**, associated to the Eq. (4) with parameters $\delta t = 0.02$, $\delta x = 4$, $\delta \theta = 2/3$, $x_{\max} = 3000$ and $\theta_{\max} = 201$. (a) Trait distribution given by the numerical simulations, at $t = 200$. (b) Trait distribution behind the propagating front given by Conjecture 1, at $t = 200$. The red line represents the approximation of the mean trait behind the propagating front given by (8), and is common to both subfigures, while the dark line is the mean trait behind the propagating front given by the simulations.

We can compare this relationship with the mean of the dispersive trait $\bar{\theta}(t)$ at the front $X(t)$, given respectively by (8) and (7):

$$\bar{\theta}(t) = \lambda^{4/5} (6X(t)^2)^{1/5} = 2\lambda\sqrt{t} = \sqrt{2t}.$$

We notice a non trivial difference between $\bar{\theta}(t)$ and $\bar{\theta}^{num}$, mainly in their prefactors ($\sqrt{2}$ and 1.02), but also in their exponents (0.5 and 0.54) (see also the gap between the red and black lines in Fig. 2). This seems partly due to numerical inaccuracies resulting

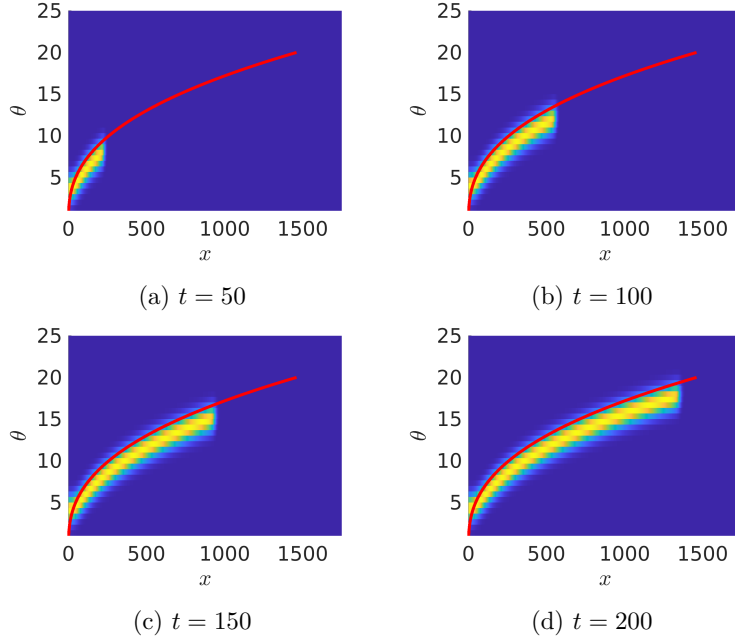


Figure 3: **Contour lines of the trait distribution during the invasion of a sexual population**, given by simulations, at (a) $t = 50$ (b) $t = 100$ (c) $t = 150$ (d) $t = 200$. The red line represents the approximation of the mean trait behind the propagating front given by (8), at time $t = 200$. The parameters are $\delta t = 0.02$, $\delta x = 4$, $\delta \theta = 2/3$, $x_{\max} = 3000$ and $\theta_{\max} = 201$.

from having a bounded trait space (thus disregarding the largest traits) and from numerical scheme errors. One can also note that the asymptotic distribution indicated by Conjecture 1 might not yet be reached at time 200 (upper time bound in our numerical simulations).

Let us turn to the description of the trait distribution behind the front. In Fig. 2, we display the contour lines of the trait distribution at time $t = 200$: subfigure (a) is the trait distribution given by the simulations, while (b) is the formal trait distribution (behind the front only) given by Conjecture 1. Our approximation appears to fit the numerical results. More precisely, the red curve, representing the mean of the dispersive trait at each position behind the front given by (8), yields a good approximation of the numerical mean of the dispersive trait. Moreover, if we represent the numerical trait distribution behind the front at multiple times (see Fig. 3), we can see that it seems to remain stationary, which is consistent with the fact that the expression of the approximation behind the front given by Conjecture 1 is independent of the time.

Fig. 4 shows the evolution of the amplitude of the trait distribution $f(t, x, \cdot)$ ahead of the front, in blue curve (log scale). We can see that it can be approximated by the red curve, which displays the prefactor of the trait distribution ahead of the front given by

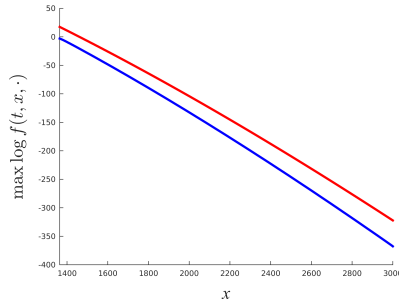


Figure 4: **Plot of logarithm of the amplitude of the distribution ahead of the front at time $t = 200$.** The blue curve represents the log of the maximum of the distribution $f(t, x, \cdot)$ of the numerical approximation given by the scheme, for different positions x located beyond the numerical value of the front position ($X^{\text{num}}(200) \approx 1400$). The red curve represents the prefactor of the trait distribution ahead of the front given by Conjecture 1. The parameters are $\delta t = 0.02$, $\delta x = 4$, $\delta \theta = 2/3$, $x_{\text{max}} = 3000$ and $\theta_{\text{max}} = 201$.

Conjecture 1, and that this approximation holds even at very low density. The difference is due to the other terms of higher power, which are neglected.

4 Formal proof of the results

This section is devoted to the formal proof of Conjecture 1. In Section 4.1, we set the self-similar variables framework suitable to capture the asymptotic invasion acceleration process. Then in Section 4.2, we formally derive an asymptotic equation that will allow us in Section 4.3 to determine the position of the front and to derive an approximation of the trait distribution $f(t, x, \theta)$ by finding a solution to the limit problem.

4.1 Preliminaries

According to the same methodology used in previous studies that model the evolution of dispersion (see for instance Bouin, Henderson, and Ryzhik 2017; Calvez, Crevat, et al. 2019; Calvez, Henderson, et al. 2018), we define the function u such that:

$$f(t, x, \theta) = \exp \left[-t u \left(s(t), t^{-5/4} x, t^{-1/2} \theta \right) \right], \quad (14)$$

where $s(t) = \log(t)$ is a time parametrization (chosen so that $ts'(t) = 1$). According to the formal arguments of Calvez, Crevat, et al. 2019, we also scale the spatial variable ($y = t^{-5/4}x$) and trait variable ($\eta = t^{-1/2}\theta$), which leads to the spatial invasion rate accelerating proportionally to $t^{5/4}$ (see Calvez, Crevat, et al. 2019 for details). Like in the latter, we recall that the power exponents are chosen so that the all biological forces

(particularly, migration and reproduction) contribute in a balanced way in the following PDE on u , satisfied for all $t \geq 0$, for all $y \in \mathbb{R}$ and for all $\eta \geq e^{-s/2}$:

$$\begin{aligned} -u(s, y, \eta) - \partial_s u(s, y, \eta) + \frac{5}{4} y \partial_y u(s, y, \eta) + \frac{\eta}{2} \partial_\eta u(s, y, \eta) \\ = \eta \left[(\partial_y u(s, y, \eta))^2 - e^{-s} \Delta_y u(s, y, \eta) \right] \\ + (I[u](s, y, \eta) - \varrho_u(s, y)), \end{aligned} \quad (15)$$

where:

$$\varrho_u(s, y) = e^{s/2} \int_{e^{-s/2}}^{\infty} \exp[-e^s u(s, y, \eta)] d\eta, \quad (16)$$

and:

$$\begin{aligned} I[u](s, y, \eta) = \frac{e^s}{\sqrt{2\pi\lambda^2} \varrho_u(s, y)} \\ \iint_{(e^{-s/2}, \infty)^2} \exp \left[e^s \left(-\frac{(\eta - \frac{\eta_1 + \eta_2}{2})^2}{2\lambda^2} + [u(s, y, \eta) - u(s, y, \eta_1) - u(s, y, \eta_2)] \right) \right] d\eta_1 d\eta_2. \end{aligned} \quad (17)$$

Henceforth, we note for the sake of clarity: $\alpha = 5/4$ and $\beta = 1/2$. We generalise also the notation $o_{\epsilon \rightarrow 0}(\epsilon^p)$ for a sequence of functions $r_\epsilon(y, \eta)$ by :

$$r_\epsilon(y, \eta) = o_{\epsilon \rightarrow 0}(\epsilon^p) \text{ if } \sup_{(y, \eta)} |\epsilon^{-p} r_\epsilon(y, \eta)| \text{ goes to } 0, \text{ as } \epsilon \text{ vanishes.}$$

Our formal aim is to determine the large time behaviour of the solution of (15), as $s \rightarrow \infty$ (which is equivalent to take $t \rightarrow \infty$).

4.2 Formal asymptotic equation

In this subsection, we will derive from (15) an asymptotic equation in the limit $s \rightarrow \infty$ that will explicit the interplay between spatial sorting and trait distribution at the front of the solution. The main idea is to perform a Taylor expansion of u . For that purpose, let us define the variation $\epsilon = e^{-s/2}$. In the line of Calvez, Garnier, and Patout 2019, we make the following ansatz:

$$u(s, y, \eta) = u_0(y, \eta) + \epsilon^2 u_1(y, \eta) + o_{\epsilon \rightarrow 0}(\epsilon^2). \quad (18)$$

In the next paragraph, we justify the following separation of trait and space variable in u_0 , where:

$$u_0(y, \eta) = b(y) + \frac{(\eta - a(y))^2}{4\lambda^2}. \quad (19)$$

where a and b are continuous and piecewise differentiable functions of the space variable. Let us interpret them.

Using the ansatz (18) and (19) in (14) yields (we recall that $\epsilon = e^{-s/2}$):

$$f(s, y, \eta) = \exp \left[-\frac{b(y)}{\epsilon^2} \right] \exp \left[-\frac{(\eta - a(y))^2}{4\lambda^2 \epsilon^2} \right] \exp \left[-u_1(y, \eta) + \underset{\epsilon \rightarrow 0}{o}(\epsilon^2) \right]. \quad (20)$$

Hence, when $s \rightarrow \infty$, the leading term of the trait distribution $\eta \mapsto f(s, y, \cdot)$ is Gaussian, and the correction is brought by a term determined by u_1 . The space dependent functions a and b crystallize the main effect of spatial sorting on the trait distribution:

- ◊ $a(y)$ gives the mean rescaled dispersal trait $\eta > 0$ at position y . It is therefore positive and satisfies the relation:

$$u_0(y, a(y)) = \min\{u_0(y, \eta), \text{ with } \eta \in (0, \infty)\};$$

- ◊ $b(y)$ determines the prefactor of this distribution: formally, we will see that if $b(y) > 0$, $\varrho_u(s, \cdot)$ vanishes when s tends to ∞ . On the contrary, the set $\{b(y) = 0\}$ is associated to that area where ϱ_u is asymptotically non-zero. In the context of a spatial invasion, it corresponds to the spatial area that has already been invaded. Hence, we are searching b such that there exists a constant y_c such that $\{b(y) = 0\} = \{y \leq y_c\}$. We can interpret y_c as the rescaled position of the front.

Finally, the space dependent functions a and b are linked to the corrector term u_1 by an asymptotic equation that we deduce from (15) (see below for the details). For y where a and b are differentiable:

$$\begin{aligned} -b(y) - \frac{(\eta - a(y))^2}{4\lambda^2} + \alpha y \left[b'(y) - a'(y) \frac{\eta - a(y)}{2\lambda^2} \right] + \beta \eta \frac{\eta - a(y)}{2\lambda^2} - \eta \left[b'(y) - a'(y) \frac{\eta - a(y)}{2\lambda^2} \right]^2 \\ = \exp \left[u_1(y, \eta) + u_1(y, a(y)) - 2u_1 \left(y, \frac{\eta + a(y)}{2} \right) \right] - \mathbf{1}_{\{y \leq y_c\}}. \end{aligned} \quad (21)$$

In the next section, we find an explicit solution to (21), which encodes the intertwined relationship between spatial sorting and trait distribution.

Explanation for the decomposition of u_0 (19). We will recall the fundamental steps, more extensively detailed formally in Bouin, Bourgeron, et al. 2018 and rigorously in Calvez, Garnier, and Patout 2019 (for a model without any spatial structure). From the Taylor expansion of u given in (18), we get the following expression for $I[u]$:

$$I[u](s, \eta, y) = \frac{1}{\epsilon \sqrt{2\pi\lambda^2}} \iint_{(\epsilon, \infty)^2} \frac{\exp \left[\frac{1}{\epsilon^2} A_{y, \eta}^0(\eta_1, \eta_2) \right] \exp \left[A_{y, \eta}^1(\eta_1, \eta_2) \right] \exp \left[\underset{\epsilon \rightarrow 0}{o}(1) \right] d\eta_1 d\eta_2}{\int_{\epsilon}^{\infty} \exp \left[-\frac{u_0(y, \eta')}{\epsilon^2} - u_1(y, \eta') \right] d\eta'},$$

where:

$$\begin{cases} A_{y, \eta}^0(\eta_1, \eta_2) = -\frac{1}{2\lambda^2} \left[\eta - \frac{\eta_1 + \eta_2}{2} \right]^2 + u_0(y, \eta) - u_0(y, \eta_1) - u_0(y, \eta_2), \\ A_{y, \eta}^1(\eta_1, \eta_2) = u_1(y, \eta) - u_1(y, \eta_1) - u_1(y, \eta_2). \end{cases}$$

Then, we have several considerations to make. First, if we assume that u_0 reaches its minimum at a non degenerated-point, then the following modified expression of the denominator:

$$\int_{\epsilon}^{\infty} \exp \left[-\frac{1}{\epsilon^2} [u_0(y, \eta') - \min u_0(y, \cdot)] - u_1(y, \eta') \right] d\eta',$$

will concentrate, as ϵ goes to 0, around the minimum of $u_0(y, \cdot)$ and have a finite limit. Therefore it is relevant to introduce it both at the numerator and the denominator:

$$\frac{1}{[\epsilon\sqrt{2\pi\lambda^2}]^2} \frac{\iint_{(\epsilon, \infty)^2} \exp \left[\frac{1}{\epsilon^2} (A_{y, \eta}^0(\eta_1, \eta_2) + \min u_0(y, \cdot)) \right] \exp \left[A_{y, \eta}^1(\eta_1, \eta_2) + \underset{\epsilon \rightarrow 0}{o}(1) \right] d\eta_1 d\eta_2}{\frac{1}{\epsilon\sqrt{2\pi\lambda^2}} \int_{\epsilon}^{\infty} \exp \left[-\frac{1}{\epsilon^2} [u_0(y, \eta') - \min u_0(y, \cdot)] - u_1(y, \eta') \right] d\eta'}.$$

As we want consequently the numerator not to diverge as $\epsilon \rightarrow 0$, we need that:

$$\forall \eta \in \mathbb{R}, \max_{(\eta_1, \eta_2)} \left[-\frac{1}{2\lambda^2} \left(\eta - \frac{\eta_1 + \eta_2}{2} \right)^2 + u_0(y, \eta) - u_0(y, \eta_1) - u_0(y, \eta_2) + \min u_0(y, \cdot) \right] = 0. \quad (22)$$

As shown in Bouin, Bourgeron, et al. 2018, thanks to some convexity arguments, this leads necessarily to choose $u_0(y, \cdot)$ as a quadratic function in η with variance λ^2 , hence (19).

Deriving the asymptotic Eq. (21) verified by $u_1(\eta, y), a(y)$ and $b(y)$. To get an asymptotic equation from (15), we still need to establish (formally) the limit of $I[u](s, y, \eta)$ as $s = -2\log(\epsilon)$ goes to ∞ , by incorporating the quadratic expression (19) of u_0 in $I[u]$. We will separate the cases of the numerator and the denominator for the sake of clarity.

According to Laplace's method, as we expect the denominator to concentrate around the minimum of u_0 , namely at $a(y)$, one can perform the change of variable $z := \frac{\eta' - a(y)}{\epsilon}$:

$$\begin{aligned} \frac{1}{\epsilon\sqrt{2\pi\lambda^2}} \int_{\epsilon}^{\infty} \exp \left[-\frac{1}{\epsilon^2} [u_0(y, \eta') - \min u_0(y, \cdot)] - u_1(y, \eta') \right] d\eta' \\ = \frac{1}{\sqrt{2\pi\lambda^2}} \int_{1-a(y)/\epsilon}^{\infty} \exp \left[-\frac{z^2}{4\lambda^2} \right] \exp [-u_1[y, a(y) + \epsilon z]] dz \xrightarrow{\epsilon \rightarrow 0} \sqrt{2} \exp [-u_1[y, a(y)]] . \end{aligned}$$

Similarly, following the analysis of the authors of Bouin, Bourgeron, et al. 2018 and Calvez, Garnier, and Patout 2019 on (22), we get that the numerator concentrates around the point $(\bar{\eta}, \bar{\eta})$, with $\bar{\eta} = \frac{\eta + a(y)}{2} > 0$, realizing its minimum. One can thus perform the change of variables $(\eta_1, \eta_2) = (\bar{\eta} + \epsilon z_1, \bar{\eta} + \epsilon z_2)$, so that a straightforward computation following the quadratic expression (19) of u_0 leads to:

$$\begin{aligned} -\frac{1}{\epsilon^2} \left[-\frac{1}{2\lambda^2} \left[\eta - \frac{\eta_1 + \eta_2}{2} \right]^2 + u_0(y, \eta) - u_0(y, \eta_1) - u_0(y, \eta_2) + \min u_0(y, \cdot) \right] \\ = \frac{1}{4\lambda^2} z_1 z_2 + \frac{3}{8\lambda^2} (z_1^2 + z_2^2), \quad (23) \end{aligned}$$

and therefore:

$$\begin{aligned} \frac{1}{[\epsilon\sqrt{2\pi\lambda^2}]^2} \iint_{(\epsilon, \infty)^2} \exp \left[\frac{1}{\epsilon^2} (A_{y, \eta}^0(\eta_1, \eta_2) + \min u_0(y, \cdot)) \right] \exp \left[A_{y, \eta}^1(\eta_1, \eta_2) + \underset{\epsilon \rightarrow 0}{o}(1) \right] d\eta_1 d\eta_2 \\ = \iint_{(1-\bar{\eta}/\epsilon, \infty)^2} \frac{\exp \left[-\frac{z_1 z_2}{4\lambda^2} - \frac{3}{8\lambda^2} (z_1^2 + z_2^2) \right]}{[\sqrt{2\pi\lambda^2}]^2} \exp [u_1(y, \eta) - u_1(y, \bar{\eta} + \epsilon z_1) - u_1(y, \bar{\eta} + \epsilon z_2)] dz_1 dz_2, \\ \xrightarrow{\epsilon \rightarrow 0} \sqrt{2} \exp [u_1(y, \eta) - 2u_1(y, \bar{\eta})] . \end{aligned}$$

We can thereby obtain the formal limit of $I[u]$:

$$I[u](s, y, \eta) \xrightarrow{s \rightarrow \infty} \exp \left[u_1(y, \eta) + u_1(y, a(y)) - 2u_1 \left(y, \frac{\eta + a(y)}{2} \right) \right].$$

Moreover, we need the formal limit of $\varrho_u(s, y)$ as $s = -2 \log(\epsilon)$ tends to ∞ :

$$\begin{aligned} \varrho_u(-2 \log(\epsilon), y) &= \frac{1}{\epsilon} \int_{\epsilon}^{\infty} \exp \left[-\frac{u(-2 \log(\epsilon), y, \eta)}{\epsilon^2} \right] d\eta, \\ &= \exp \left[-\frac{b(y)}{\epsilon^2} \right] \frac{1}{\epsilon} \int_{\epsilon}^{\infty} \exp \left[-\frac{(\eta - a(y))^2}{4\lambda^2 \epsilon^2} \right] \exp \left[-u_1(y, \eta) + \underset{\epsilon \rightarrow 0}{o}(1) \right] d\eta, \\ &= \exp \left[-\frac{b(y)}{\epsilon^2} \right] \int_{1 - \frac{a(y)}{\epsilon}}^{\infty} \exp \left[-\frac{z^2}{4\lambda^2} \right] \exp \left[-u_1(y, a(y) + \epsilon z) + \underset{\epsilon \rightarrow 0}{o}(1) \right] dz. \end{aligned}$$

Hence, formally, we get:

$$\varrho_u(-2 \log(\epsilon), y) \xrightarrow{\epsilon \rightarrow 0} \mathbf{1}_{\{b(y)=0\}} 2\sqrt{\pi}\lambda \exp[-u_1(y, a(y))].$$

By integrating all these formal computations in (15), we formally obtain an asymptotic equation satisfied by a , b and u_1 , where a and b are differentiable:

$$\begin{aligned} -b(y) - \frac{(\eta - a(y))^2}{4\lambda^2} + \alpha y \left[b'(y) - a'(y) \frac{\eta - a(y)}{2\lambda^2} \right] + \beta \eta \frac{\eta - a(y)}{2\lambda^2} - \eta \left[b'(y) - a'(y) \frac{\eta - a(y)}{2\lambda^2} \right]^2 \\ = \exp \left[u_1(y, \eta) + u_1(y, a(y)) - 2u_1 \left(y, \frac{\eta + a(y)}{2} \right) \right] \\ - \mathbf{1}_{\{b(y)=0\}} 2\sqrt{\pi}\lambda \exp[-u_1(y, a(y))]. \end{aligned}$$

As we are describing a front propagation, we are looking for a and b continuous on \mathbb{R} and differentiable everywhere but not necessarily at the front position (to be determined):

$$y_c = \sup\{y, b(y) = 0\}.$$

For such functions a and b , we have by evaluating the latter at $\eta = a(y)$ for $y < y_c$:

$$2\sqrt{\pi}\lambda \exp[-u_1(y, a(y))] = 1.$$

Hence, for $y \neq y_c$ and $\eta \in J_y$ (subset of \mathbb{R}_+^* to be determined), we consider the asymptotic Eq. (21):

$$\begin{aligned} -b(y) - \frac{(\eta - a(y))^2}{4\lambda^2} + \alpha y \left[b'(y) - a'(y) \frac{\eta - a(y)}{2\lambda^2} \right] + \beta \eta \frac{\eta - a(y)}{2\lambda^2} - \eta \left[b'(y) - a'(y) \frac{\eta - a(y)}{2\lambda^2} \right]^2 \\ = \exp \left[u_1(y, \eta) + u_1(y, a(y)) - 2u_1 \left(y, \frac{\eta + a(y)}{2} \right) \right] - \mathbf{1}_{\{y < y_c\}}. \end{aligned}$$

4.3 Resolution of the asymptotic Eq. (21)

Let us define for $y \neq y_c$, $\eta > 0$:

$$g(y, \eta) := -b(y) - \frac{(\eta - a(y))^2}{4\lambda^2} + \alpha y \left[b'(y) - a'(y) \frac{\eta - a(y)}{2\lambda^2} \right] \\ + \beta \eta \frac{\eta - a(y)}{2\lambda^2} - \eta \left[b'(y) - a'(y) \frac{\eta - a(y)}{2\lambda^2} \right]^2 + \mathbf{1}_{\{y < y_c\}}.$$

Let us fix $y \neq y_c$. For $\eta > 0$ such that $g(y, \eta) > 0$, we can reformulate (21) as:

$$T_y(\eta) = L_y(u_1)(\eta), \quad (24)$$

where:

$$T_y(\eta) = \log [g(y, \eta)],$$

and:

$$L_y(u_1) : \eta \mapsto u_1(y, \eta) + u_1(y, a(y)) - 2u_1\left(y, \frac{\eta + a(y)}{2}\right).$$

Eq. (24) suggests that a , b and y_c are to be chosen so that T_y lies in the image of the linear operator L_y . One can notice that the kernel of L_y is composed of the linear functions, hence:

$$\dim \ker (L_y) = 2.$$

Heuristically, the image of L_y is orthogonal to a two dimensional space, which is generated by $\delta_{a(y)}$ and $\delta'_{a(y)}$. More precisely, following Calvez, Garnier, and Patout 2019, one can show that if T_y verifies:

$$\begin{cases} T_y(a(y)) = 0, \\ T'_y(a(y)) = 0, \end{cases} \quad (25)$$

then the following sum converges:

$$u_y : \eta \mapsto \sum_{k=0}^{\infty} 2^k T_y \left[a(y) + (\eta - a(y)) 2^{-k} \right], \quad (26)$$

and $L_y(u_y) = T_y$.

Hence, we first need to solve (25), that is to find $y_c > 0$, $(a, b) \in C^0(\mathbb{R}) \cap C^1(\mathbb{R} \setminus \{y_c\})$, such that:

$$\forall y \neq y_c, \quad \begin{cases} -b(y) + \alpha y b'(y) - a(y)(b'(y))^2 + \mathbf{1}_{\{y < y_c\}} = 1, \\ -\alpha y a'(y) + \beta a(y) - 2\lambda^2 (b'(y))^2 + 2a(y)b'(y)a'(y) = 0. \end{cases} \quad (27)$$

Here, we present an explicit solution to (27):

Proposition 1. *Let us define:*

$$y_c = 4\sqrt{\frac{\lambda}{3}}, \quad a : y \mapsto \begin{cases} \lambda^{4/5} 6^{1/5} y^{2/5}, & \text{if } y \leq y_c, \\ \left(\frac{3\lambda^2}{2}\right)^{1/3} y^{2/3}, & \text{if } y > y_c, \end{cases}$$

and:

$$b : y \mapsto \begin{cases} 0, & \text{if } y \leq y_c, \\ \left(\frac{3}{\lambda^2}\right)^{2/3} y^{4/3} - 1, & \text{if } y > y_c. \end{cases}$$

Then $a, b \in C^0(\mathbb{R}) \cap C^1(\mathbb{R} \setminus \{y_c\})$ and y_c, a and b are solutions of (27).

Remark 1. *The functions a, b and y_c given in the previous proposition are the only solutions of (27) of the form $a(y) = Cy^m, b(y) = Ky^n - 1$ that are positive for $y > y_c$ and continuous in y_c .*

To derive a solution for (21) from Proposition 1, one still has to define $T_y(\eta)$, which requires $g(y, \eta) > 0$. As $g(y, \cdot)$ is a three order polynomial in η with a negative leading coefficient, it is not positive as η becomes large so we can not define T_y on \mathbb{R}_+ . However, a, b and y_c are solutions of (27), which is equivalent to:

$$g(y, a(y)) = 1, \quad \partial_\eta g(y, a(y)) = 0.$$

We aim therefore at solving (21) locally in η around $a(y)$:

Proposition 2. *Let a, b and y_c be as in Proposition 1. Then, there exists J_0 an interval centered in 1 such that, for all $y \neq y_c, \eta > 0$ such that $\frac{\eta}{a(y)} \in J_0$, we have $g(y, \eta) > 0$. Moreover, for $y \neq y_c, T_y = \log(g(y, \cdot))$ is well defined on $a(y) \cdot J_0$ and for all $J \subset J_0$ open interval centered in 1:*

- ◊ for $y < y_c$ and $\eta \in a(y) \cdot J$, the series defined in (26) converges and is bounded uniformly with regard to η and y and the bound is of the form $A|J|^2$.
- ◊ for $y > y_c$ and $\eta \in a(y) \cdot J$, the series defined in (26) converges and is bounded uniformly with regard to η , and the bound is of the form: $B|J|^2 y^{8/3}$.

Proof. Since $g(y, \cdot)$ is a polynomial of order three in η such that:

$$g(y, a(y)) = 1, \quad \partial_\eta g(y, a'(y)) = 0,$$

we can define P_y polynomial of order three such that:

$$\forall \eta > 0, \quad g(y, \eta) = 1 - P_y \left(\frac{\eta}{a(y)} \right).$$

As $P_y(1) = P'_y(1) = 0$, we get:

$$P_y(X) = (X - 1)^2 [\gamma X + P_y(0)],$$

where $\gamma > 0$ is the leading coefficient of P_y .

We next compute, for $y \neq y_c$ (by continuity for $P_y(0)$):

$$\gamma = \frac{a'(y)^2 a(y)^3}{4\lambda^4}, \quad P_y(0) = b(y) + \frac{a(y)^2}{4\lambda^2} - \alpha y \left[b'(y) + a'(y) \frac{a(y)}{2\lambda^2} \right] + \mathbf{1}_{\{y > y_c\}}.$$

Hence (adopting the notations K_{a-}, K_{a+} and K_b such that for $y < y_c, a(y) = K_{a-} y^{2/5}$ and for $y > y_c, a(y) = K_{a+} y^{2/3}, b(y) = K_b y^{4/3} - 1$ – see the previous proposition):

◇ for $y < y_c$, $\gamma = \frac{a(y)^5}{25y^2\lambda^4} = \frac{K_{a^-}^5}{25\lambda^4}$ and:

$$P_y(0) = \frac{a^2}{4\lambda^2} - \frac{\alpha a'(y)ya(y)}{2\lambda^2} = \frac{a^2}{4\lambda^2} - \frac{5}{4} \cdot \frac{2a^2}{10\lambda^2} = 0.$$

So, in that case, $P_y = \frac{K_{a^-}^5}{25\lambda^4}(X-1)^2X := P(X)$ does not depend on y . As $P(1) = 0$, there exists $\delta \in (0, 1)$ such that for all $y < y_c$ and $\eta \in]a(y)(1-\delta), a(y)(1+\delta)[$, $P\left(\frac{\eta}{a(y)}\right) < 1$, hence $g(y, \eta) > 0$.

◇ for $y > y_c$, $\gamma = \frac{4}{9} \frac{a(y)^5}{4y^2\lambda^4} = \frac{K_{a^+}^5}{9\lambda^4} y^{4/3}$ and:

$$\begin{aligned} P_y(0) &= (b(y) + 1) - \frac{5}{3}(1 + b(y)) + \frac{a(y)^2}{4\lambda^2} - \frac{5a(y)^2}{12\lambda^2}, \\ &= -y^{4/3} \left[\frac{K_{a^+}^2}{6\lambda^2} + \frac{2K_b}{3} \right] = -\gamma y^{4/3} \left[\frac{3\lambda^2}{2K_{a^+}^3} + \frac{6K_b\lambda^4}{K_{a^+}^5} \right], \\ &= -\gamma y^{4/3} \left[1 + 6 \times \frac{3^{2/3}\lambda^4 2^{5/3}}{2^{8/3}\lambda^{12/3} 3^{5/3}} \right] = -2\gamma y^{4/3}. \end{aligned}$$

Hence: $P_y(X) = \gamma y^{4/3}(X-1)^2(X-2)$, thus: $\forall y > y_c, \forall \eta \in]0, 2a(y)[$, $g(y, \eta) > 1 > 0$.

That proves the first part of the proposition. Let us call J_0 a closed interval centered in 1 on which, for all $y \neq y_c$, $g(y, \cdot)$ is positive, and on which T_y is therefore well-defined.

Let us now consider $J \subset J_0$ an open interval centered in 1. For $y \neq y_c$, $\eta \in a(y) \cdot J$, let us define, for $k \in \mathbb{N}$:

$$\eta_k := a(y) + \frac{\eta - a(y)}{2^k}.$$

Next, as $T_y(a(y)) = T'(a(y)) = 0$, we get the following:

$$2^k T_y(\eta_k) = 2^k \int_{a(y)}^{\eta_k} T_y''(t) \frac{\eta_k - t}{2} dt.$$

With the change of variables $s = 2^k(t - a(y))$, we get:

$$2^k T_y(\eta_k) = \int_0^{\eta - a(y)} T_y''(a(y) + s2^{-k}) \frac{\eta - a(y) - s}{2^k} ds. \quad (28)$$

T_y'' is continuous on $a(y) \cdot J$, so the latter ensures that $\sum_{k \geq 0} 2^k T(\eta_k)$ converges for all $\eta \in a(y) \cdot J$.

Finally, for $y \neq y_c$, we need to uniformly bound $\sum_{k \geq 0} 2^k T(\eta_k)$ with regard to $\eta \in a(y) \cdot J$. For $y < y_c$, from the first part of the proof, we have:

$$\forall \eta \in a(y) \cdot J, \quad T_y(\eta) = \log \left(1 - P \left(\frac{\eta}{a(y)} \right) \right),$$

with $P(X) = \gamma X(X-1)^2$ and γ independent of y and η . Setting:

$$\begin{aligned} F &: J \rightarrow \mathbb{R}, \\ x &\mapsto \log(1 - P(x)), \end{aligned}$$

we dispose of a smooth function, independent from y and η , such that:

$$\forall \eta \in a(y) \cdot J, \quad T_y(\eta) = F\left(\frac{\eta}{a(y)}\right),$$

and therefore $T_y''(\eta) = F''(\eta/a(y))/a(y)^2$. Following (28), we get (writing $|J|$ as the length of J):

$$\forall y < y_c, \eta \in a(y) \cdot J, \quad \sum_{k \geq 0} |2^k T_y(\eta_k)| \leq \sum_{k \geq 0} 2^{-(k+1)} \|F''\|_{\infty, J} \frac{(\eta - a(y))^2}{a(y)^2} \leq |J|^2 \|F''\|_{\infty, J_0}.$$

For $y > y_c$, we have from above:

$$\forall \eta \in a(y) \cdot J, \quad T_y(\eta) = \log\left(1 - y^{4/3} Q\left(\frac{\eta}{a(y)}\right)\right),$$

with $Q(X) = \gamma_Q(X-1)^2(X-2)$ (γ_Q a constant independent of y and η). A straightforward calculus leads to:

$$T_y''(\eta) = -\frac{y^{4/3}}{a(y)^2} \left[\frac{Q''\left(\frac{\eta}{a(y)}\right)}{1 - y^{4/3} Q\left(\frac{\eta}{a(y)}\right)} + y^{4/3} \frac{Q'\left(\frac{\eta}{a(y)}\right)^2}{\left(1 - y^{4/3} Q\left(\frac{\eta}{a(y)}\right)\right)^2} \right].$$

We recall that, additionally, for $y > y_c$ and $\eta \in a(y) \cdot J$, we have: $1 - y^{4/3} Q\left(\frac{\eta}{a(y)}\right) > 1$. Hence, from (28), we get:

$$\begin{aligned} \forall y > y_c, \forall \eta \in a(y) \cdot J, \quad \sum_{k \geq 0} |2^k T_y(\eta_k)| &\leq y^{4/3} |J|^2 \left[\|Q''\|_{\infty, J} + y^{4/3} \|Q'^2\|_{\infty, J} \right] \\ &\leq y^{8/3} |J|^2 \left[\frac{\|Q''\|_{\infty, J_0}}{y_c^{4/3}} + \|Q'^2\|_{\infty, J_0} \right]. \end{aligned}$$

□

The last proposition allows us to complete our solution for (21) for $y \neq y_c$ and $\eta \in a(y) \cdot J$, by defining:

$$u_1 : (y, \eta) \mapsto \sum_{k \geq 0} 2^k T_y(a(y) + (\eta - a(y)) 2^{-k}).$$

It also highlights the fact that this solution is local in trait around the mean trait $a(y)$. Finally, we use it in Conjecture 1 to specify the magnitude of the error terms in our approximation at large times.

5 Discussion

Contributions In this paper, we have developed a different framework than the one used for the study of asexual populations (N. Berestycki, Mouhot, and Raoul 2015; Bouin, Henderson, and Ryzhik 2017; Calvez, Henderson, et al. 2018) by using a mixing operator to analyze the behaviour of the propagation front for sexual population. We have formally found an explicit approximation of the trait distribution during the invasion by finding a solution to the limit problem at large times. These formal computations have been numerically compared to the

solution of (4) and thus confirmed. All the computations have been made after having rescaled the partial differential Eq. (2). By a variable change, we have that, for all growth rate at low density $r > 0$, carrying capacity $K > 0$ and segregational variance $\lambda^2 > 0$, for a population with dispersive traits $\theta \geq \theta_{\min} > 0$, the density f can be approximated at large time $t > 0$ by:

$$f(t, x, \theta) \approx \frac{K}{\theta_{\min}} \begin{cases} \exp \left[-\frac{1}{4\lambda^2} \left[\theta - \lambda^{4/5} (6rx^2)^{1/5} \right]^2 \right], & \text{for } x \leq y_c t^{5/4}, \\ \exp \left[rt - \left(\frac{9x^4}{256\lambda^2 t^2} \right)^{1/3} \right] \exp \left[-\frac{1}{4\lambda^2} \left[\theta - \left(\frac{3\lambda^2 x^2}{2t} \right)^{1/3} \right]^2 \right], & \\ & \text{for } x \geq y_c t^{5/4}. \end{cases}$$

with:

$$y_c = y_c \sqrt{\frac{\theta_{\min}}{r}} r^{5/4} = 4 \left[\frac{\lambda}{3} \right]^{1/2} \sqrt{\theta_{\min}} r^{3/4} = 4 \left[\frac{\lambda}{3} \right]^{1/2} r^{3/4}.$$

Difference in acceleration rate between asexual and sexual invasive populations Our study shows that the effect of spatial sorting only, through the evolution of dispersion, accelerates the speed at which a sexual population invades. The rate of this acceleration, of $t^{5/4}$, is lower than when considering the influence of the same phenomenon on asexual populations ($t^{3/2}$, see N. Berestycki, Mouhot, and Raoul 2015; Bouin, Henderson, and Ryzhik 2017; Calvez, Henderson, et al. 2018). Mathematically, the blending inheritance property of the infinitesimal model operator reduces the effect of the spatial sorting by crossing extremely dispersive individuals with less dispersive ones, which does not happen for individuals reproducing clonally.

Extension: Shape of the front However, there are still structural questions to answer on the asymptotic behaviour of the front that we can observe numerically. For instance, the additional Fig. 5 allows us to study the deformation of the front propagation, more precisely the shape of the transition front. In Fig. 5 (a), the spatial distribution ϱ is displayed with respect to a re-centered scale in:

$$X_{1/2}(t) = \sup\{x \in \mathbb{R}, \varrho(t, x) = 1/2\}. \quad (29)$$

We can observe a flattening of the front shape, as $t \rightarrow +\infty$. More precisely, Fig 5 (b), displaying ϱ with respect to the re-scaled variable $(x - X_{1/2}(t)) t^{-1/4}$, shows that the shape of the front seems to flatten at order $t^{1/4}$, as the different curves overlap.

Expansion load Here, we consider only a trait linked to the dispersive ability, thus isolating the sole effect of spatial sorting in range expansions, for which there existed no previous precise results. By doing so, our model does not account for any process of selection by adaptation to the local environment. However, in cases of fast range expansion, a phenomenon called the expansion load can occur Peischl, Dupanloup, et al. 2013. As the density of individuals at the front is low, the effective strength of

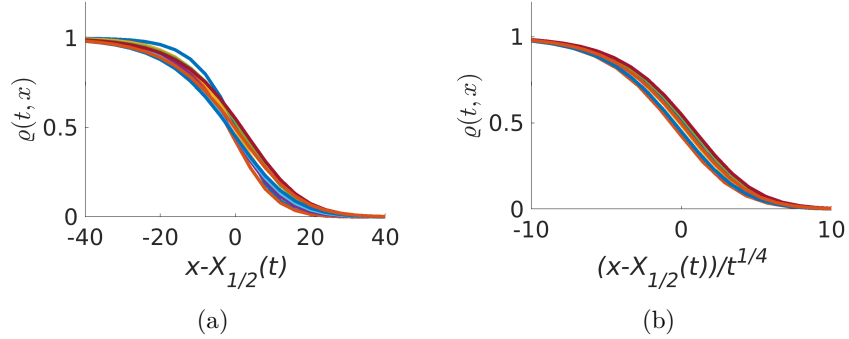


Figure 5: **Plots of the density $\varrho(t, \cdot)$ of a sexual population, with respect to re-centered variables.** The two plots show the evolution of the population density, associated to (4), for successive times at regular intervals from $t = 20$ to $t = 200$, with respect to (a) the re-centered variable $x - X_{1/2}(t)$, and (b) to the re-scaled variable $(x - X_{1/2}(t))t^{-1/4}$, with $X_{1/2}(t)$ defined in (29). The parameters are $\delta t = 0.02$, $\delta x = 4$, $\delta \theta = 2/3$, $x_{\max} = 3000$ and $\theta_{\max} = 201$. Note that the x -axis are different between the two plots, for the sake of clarity.

natural selection is reduced allowing deleterious mutations to accumulate at the front. That would eventually undermine the invasion process by reducing the fitness of leading individuals (see Burton, B. L. Phillips, and Travis 2010), with the potential effect of slowing down the speed of the front in comparison to the asymptotic formal result of our study. Nevertheless, the clear relationship between the effect of spatial sorting and expansion load is yet to be explored, as a recent analysis using a discrete space framework seems to indicate that the evolution of dispersal rate can prevent expansion load in certain cases (see Peischl and Gilbert 2020). By isolating the effect of spatial sorting, our study can therefore constitute a first step in understanding the intricate relationship between the evolution of dispersion and of life history traits, ultimately providing tools to analyse the source of variability in range expansions (see Williams, Hufbauer, and Miller 2019).

Because the formal computations ignore competition ahead of the front, even though the simulations seems to validate our results, this paper has to be seen as a premise for a consistent and rigorous proof for this problem.

Acknowledgement

This project has received funding from the European Research Council (ERC) under the European Union’s Horizon 2020 research and innovation program (grant agreement No 639638) and from the ANR projects NONLOCAL (ANR-14-CE25-0013) and RESISTE (ANR-18-CE45-0019).

Special thanks to Vincent Calvez and Gaël Raoul for the supervision of this CEM-

RACS project, and to Joachim Crevat for his central role in the genesis of this work. Thanks also to Vincent Calvez, Sepideh Mirrahimi, Lionel Roques, Joachim Crevat, Barbara Neto-Bradley, Linnéa Sandell, Gil Henriques, Sarah Otto and Ailene Macpherson for helpful comments.

References

- [AW78] D G Aronson and H F Weinberger. “Multidimensional nonlinear diffusion arising in population genetics”. In: Advances in Mathematics 30.1 (1978), pp. 33–76.
- [Ber+12] C Berthouly-Salazar et al. “Spatial Sorting Drives Morphological Variation in the Invasive Bird, *Acridotheris tristis*”. In: PLOS ONE 7.5 (2012), pp. 1–9. DOI: [10.1371/journal.pone.0038145](https://doi.org/10.1371/journal.pone.0038145).
- [BEV17] N H Barton, A M Etheridge, and A Véber. “The infinitesimal model: Definition, derivation, and implications”. In: Theoretical Population Biology 118 (Dec. 2017), pp. 50–73. ISSN: 00405809. DOI: [10.1016/j.tpb.2017.06.001](https://doi.org/10.1016/j.tpb.2017.06.001).
- [BHK17] G Birzu, O Hallatschek, and K S Korolev. “Neither pulled nor pushed: Genetic drift and front wandering uncover a new class of reaction-diffusion waves”. In: arXiv preprint arXiv:1709.01601 (2017).
- [BHN08] H Berestycki, F Hamel, and G Nadin. “Asymptotic spreading in heterogeneous diffusive excitable media”. In: Journal of Functional Analysis 255.9 (2008), pp. 2146–2189.
- [BHR17] E Bouin, C Henderson, and L Ryzhik. “Super-linear spreading in local and non-local cane toads equations”. In: Journal de mathématiques Pures et Appliquées 108.5 (2017), pp. 724–750.
- [BMR15] N Berestycki, C Mouhot, and G Raoul. “Existence of self-accelerating fronts for a non-local reaction-diffusion equations”. In: arXiv preprint arXiv:1512.00903 (2015).
- [Bou+12] E Bouin, V Calvez, et al. “Invasion fronts with variable motility: Phenotype selection, spatial sorting and wave acceleration”. In: Comptes Rendus Mathématique 350.15–16 (Aug. 2012), pp. 761–766. ISSN: 1631073X. DOI: [10.1016/j.crma.2012.09.010](https://doi.org/10.1016/j.crma.2012.09.010).
- [Bou+18] E Bouin, T Bourgeron, et al. “Equilibria of quantitative genetics models beyond the Gaussian approximation I : maladaptation to a changing environment”. In: in preparation (2018).
- [BPT10] O J Burton, B L Phillips, and J M J Travis. “Trade-offs and the evolution of life-histories during range expansion”. In: Ecology Letters 13.10 (2010), pp. 1210–1220. DOI: [10.1111/j.1461-0248.2010.01505.x](https://doi.org/10.1111/j.1461-0248.2010.01505.x). eprint: <https://onlinelibrary.wiley.com/doi/pdf/10.1111/j.1461-0248.2010.01505.x>. URL: <https://onlinelibrary.wiley.com/doi/abs/10.1111/j.1461-0248.2010.01505.x>.

- [Bul72] M G Bulmer. “The genetic variability of polygenic characters under optimizing selection, mutation and drift”. In: Genetical Research 19.01 (Feb. 1972), p. 17. ISSN: 0016-6723, 1469-5073. DOI: [10.1017/S0016672300014221](https://doi.org/10.1017/S0016672300014221).
- [Cal+18] V Calvez, C Henderson, et al. Non-local competition slows down front acceleration during dispersal 2018. arXiv: [1810.07634](https://arxiv.org/abs/1810.07634) [[math.AP](#)].
- [Cal+19] V Calvez, J Crevat, et al. “Influence of the mode of reproduction on dispersal evolution during species invasion”. In: ESAIM: Proceedings and Surveys (2019). Accepted.
- [CGP19] V Calvez, J Garnier, and F Patout. “Asymptotic analysis of a quantitative genetics model with nonlinear integral operator”. In: Journal de l’Ecole polytechnique — Mathématiques 6 (2019), pp. 537–579. ISSN: 2270-518X. DOI: [10.5802/jep.100](https://doi.org/10.5802/jep.100).
- [Fis19] R A Fisher. “The correlation between relatives on the supposition of Mendelian inheritance”. In: Earth and Environmental Science Transactions of the Royal Society of London 52.2 (1919), pp. 399–433.
- [FZ11] J Fang and X Zhao. “Monotone wavefronts of the nonlocal Fisher–KPP equation”. In: Nonlinearity 24.11 (2011), p. 3043.
- [Gou00] S A Gourley. “Travelling front solutions of a nonlocal Fisher equation”. In: Journal of mathematical biology 41.3 (2000), pp. 272–284.
- [GVA06] S Genieys, V Volpert, and P Auger. “Pattern and waves for a model in population dynamics with nonlocal consumption of resources”. In: Mathematical Modelling of Natural Phenomena 1.1 (2006), pp. 63–80.
- [HR14] F Hamel and L Ryzhik. “On the nonlocal Fisher–KPP equation: steady states, spreading speed and global bounds”. In: Nonlinearity 27.11 (2014), p. 2735.
- [Lan78] K Lange. “Central limit theorems of pedigrees”. In: Journal of Mathematical Biology 6.1 (June 1978), pp. 59–66. ISSN: 0303-6812, 1432-1416. DOI: [10.1007/BF02478517](https://doi.org/10.1007/BF02478517).
- [MR13] S Mirrahimi and G Raoul. “Dynamics of sexual populations structured by a space variable and a phenotypical trait”. In: Theoretical population biology 84 (2013), pp. 87–103.
- [Pei+13] S Peischl, I Dupanloup, et al. “On the accumulation of deleterious mutations during range expansions”. In: Molecular Ecology 22.24 (Dec. 2013), pp. 5972–5982. ISSN: 09621083. DOI: [10.1111/mec.12524](https://doi.org/10.1111/mec.12524).
- [PG20] S Peischl and K J Gilbert. “Evolution of dispersal can rescue populations from expansion load”. In: The American Naturalist 195.2 (2020), pp. 000–000.
- [Phi+06] B Phillips et al. “Invasion and the evolution of speed in toads”. In: Nature (2006).

- [Rao17] G Raoul. “Macroscopic limit from a structured population model to the Kirkpatrick-Barton model”. In: arXiv:1706.04094 [math] (June 2017). arXiv: 1706.04094. URL: <http://arxiv.org/abs/1706.04094>.
- [SBP11] R Shine, G P Brown, and B L Phillips. “An evolutionary process that assembles phenotypes through space rather than through time”. In: Proceedings of the National Acad 108.14 (2011), pp. 5708–5711.
- [TB94] M Turelli and N H Barton. “Genetic and statistical analyses of strong selection on polygenic traits: what, me normal?” In: Genetics 138.3 (1994), pp. 913–941.
- [TD02] J M J Travis and C Dytham. “Dispersal evolution during invasions”. In: Evolutionary Ecology Research 4.8 (2002), pp. 1119–1129.
- [Tho+01] C D Thomas et al. “Ecological and evolutionary processes at expanding range margins”. In: Nature 411.6837 (2001), pp. 577–581.
- [Tra+09] J M J Travis, K Mustin, et al. “Accelerating invasion rates result from the evolution of density-dependent dispersal”. In: Journal of theoretical biology 259.1 (2009), pp. 151–158.
- [Tuf00] J Tufto. “Quantitative genetic models for the balance between migration and stabilizing selection”. In: Genetical Research 76.3 (Dec. 2000), pp. 285–293. ISSN: 0016-6723, 1469-5073. DOI: [10.1017/S0016672300004742](https://doi.org/10.1017/S0016672300004742).
- [Tur17] M Turelli. “Commentary: Fisher’s infinitesimal model: A story for the ages”. In: Theoretical Population Biology 118 (Dec. 2017), pp. 46–49. ISSN: 00405809. DOI: [10.1016/j.tpb.2017.09.003](https://doi.org/10.1016/j.tpb.2017.09.003).
- [WHM19] J L Williams, R A Hufbauer, and T E X Miller. “How Evolution Modifies the Variability of Range Expansion”. In: Trends in Ecology & Evolution 34.10 (2019), pp. 903–913. ISSN: 0169-5347. DOI: <https://doi.org/10.1016/j.tree.2019.05.012>.

Supplementary Materials: Front propagation of a sexual population with evolving dispersion: a formal analysis ^{*}

Léonard Dekens[†]

Florian Lavigne [‡]

January 1, 2022

1 Simulations with a different initial distribution

In this section, we explore the robustness of the numerical confirmation of our approximation drawn in the associated article, with regard to the initial conditions. We hereby present the simulations given by the explicit Euler scheme, with the same model parameters as for the figures in the associated article. However, we assume that the initial distribution is a Dirac distribution at $x = 0$ and $\theta = 1$.

The same conclusions seem to hold: at large time t , this invasion seems to follow the same evolution as when being initially normally distributed (*cf.* the associated article). More precisely, we can see that the propagating front accelerates (see Fig 1 (a)) and that the acceleration in space can be quantified similarly: $X(t) = y_c t^{5/4}$, with $y_c > 0$.

Fig. 2 displays the numerical solution of our differential equation with a Dirac initial distribution for successive times. It is compared to the mean of the dispersive trait (red line) derived from the asymptotic approximation stated in Conjecture 1. Behind the front, the distribution seems to be stationary at large time.

2 Simulations with a different value for r

This supplementary material shows the simulations of the invasion of a sexual population, initially gaussian distributed. We change the value of the growth rate at low density: we take $r = 0.1$.

As for the other cases, the propagating front accelerates (Fig. 3). The front position is given by:

$$X^{num}(t) = y_c(r = 0.1)t^{5/4}, \quad \text{for } y_c^{num}(r = 0.1) > 0.$$

^{*}European Research Council (ERC) under the European Union's Horizon 2020 research and innovation program (grant agreement No 639638) and the ANR projects NONLOCAL (ANR-14-CE25-0013) and RESISTE (ANR-18-CE45-0019).

[†]Institut Camille Jordan, UMR5208 UCBL/CNRS, Université de Lyon; INRIA, Dracula Team. (dekens@math.univ-lyon1.fr).

[‡]Aix Marseille Univ, CNRS, Centrale Marseille, I2M, Marseille, France (florian.lavigne@univ-amu.fr, florian.lavigne@inra.fr).

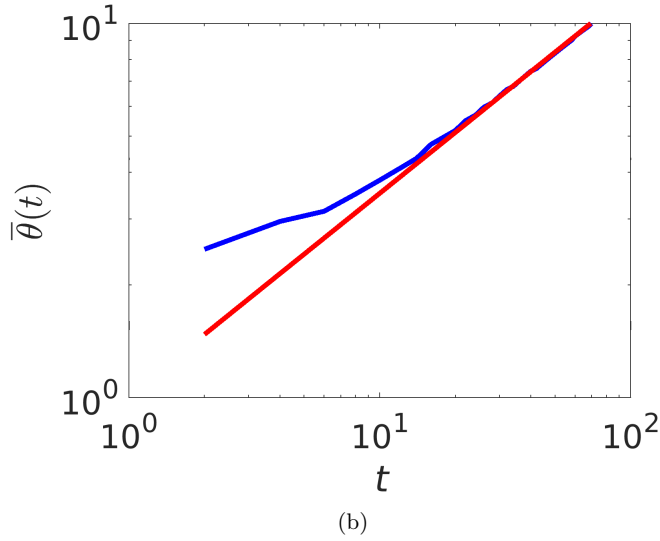
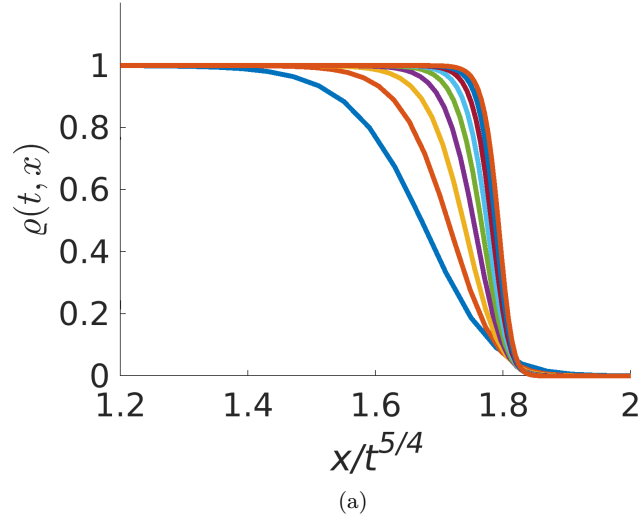


Figure 1: **Simulations of the invasion of a sexual population, initially distributed according to a Dirac distribution**, with parameters $\delta t = 0.02$, $\delta x = 4$, $\delta\theta = 2/3$, $x_{\max} = 3000$ and $\theta_{\max} = 201$. (a) Plot of the population size $\varrho(t, \cdot)$ for successive fixed times at regular intervals from $t = 20$ to $t = 200$, with respect to the auto-similar variable $xt^{-5/4}$. (b) Plot of the mean of the dispersive trait $\bar{\theta}^{num}(t)$ at the front position with respect to time (blue curve) and of the function $t \rightarrow 1.02t^{0.54}$, given by a linear regression with $R^2 = 1$ (red curve), in log – log scale.

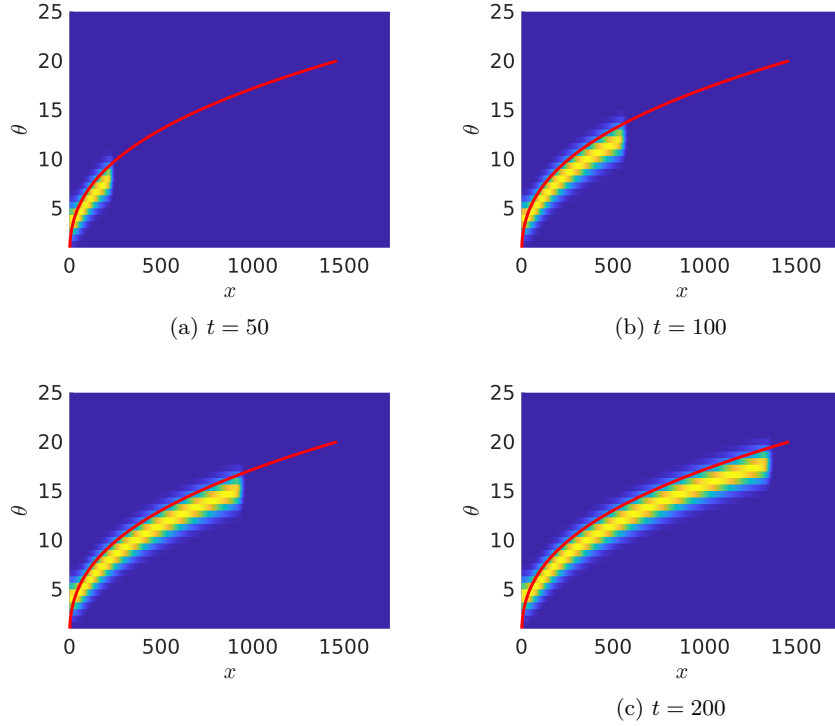


Figure 2: **Contour lines of the trait distribution during the invasion of a sexual population, initially distributed according to a Dirac distribution**, given by simulations, at (a) $t = 50$ (b) $t = 100$ (c) $t = 150$ (d) $t = 200$. The parameters are $\delta t = 0.02$, $\delta x = 4$, $\delta \theta = 2/3$, $x_{\max} = 3000$ and $\theta_{\max} = 201$. The red line represents the approximation of the mean trait behind the propagating front.

As seen in the article, the constant $y_c^{num} \approx 0.3$ depends on the growth rate at low density (r). We have already discussed about the general case (with a general coefficient r). We have guessed that the front at time $t > 0$ is at the position:

$$X(t) = 4 \left(\frac{\lambda}{3} \right)^{1/2} r^{3/4} t^{5/4} = \frac{2}{\sqrt{3}} \frac{t^{5/4}}{5^{3/4}} \approx 0.35 t^{5/4},$$

which is less consistent with our simulations (maybe because the time is not large enough). Thus the growth rate at low density r is stronger, the invasion is faster: when individuals have more children, the population can invade faster areas. We present also the evolution of the invasion in Fig. 2.

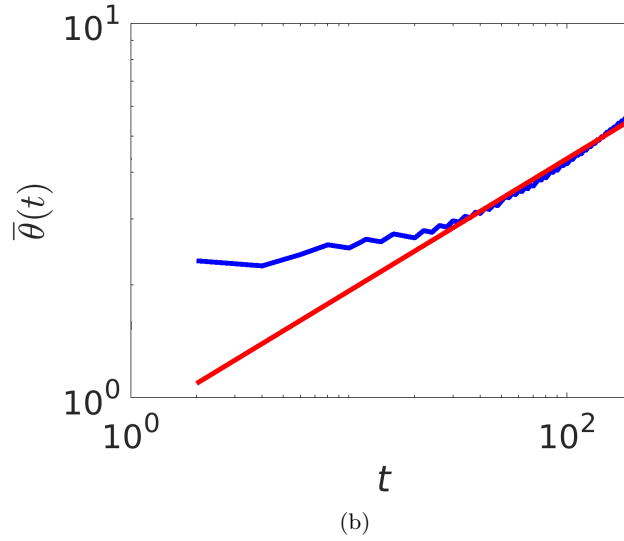
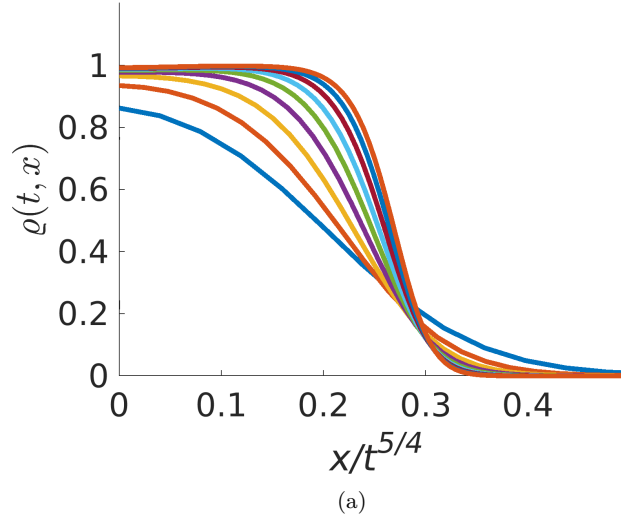


Figure 3: **Simulations of the invasion of a sexual population, initially gaussian distributed, with a different growth rate at low density ($r = 0.1$),** with parameters $\delta t = 0.02$, $\delta x = 4$, $\delta \theta = 2/3$, $x_{\max} = 3000$ and $\theta_{\max} = 201$. (a) Plot of the population size $\varrho(t, \cdot)$ for successive fixed times at regular intervals from $t = 20$ to $t = 200$, with respect to the auto - similar variable $xt^{-5/4}$. (b) Plot of the mean of the dispersive trait $\bar{\theta}^{num}(t)$ at the front position with respect to time (blue curve) and of the function $t \rightarrow 0.85t^{0.35}$ (red curve), in log - log scale. The function $t \rightarrow 0.85t^{0.35}$ is given by a linear regression, with $R^2 = 0.983$.

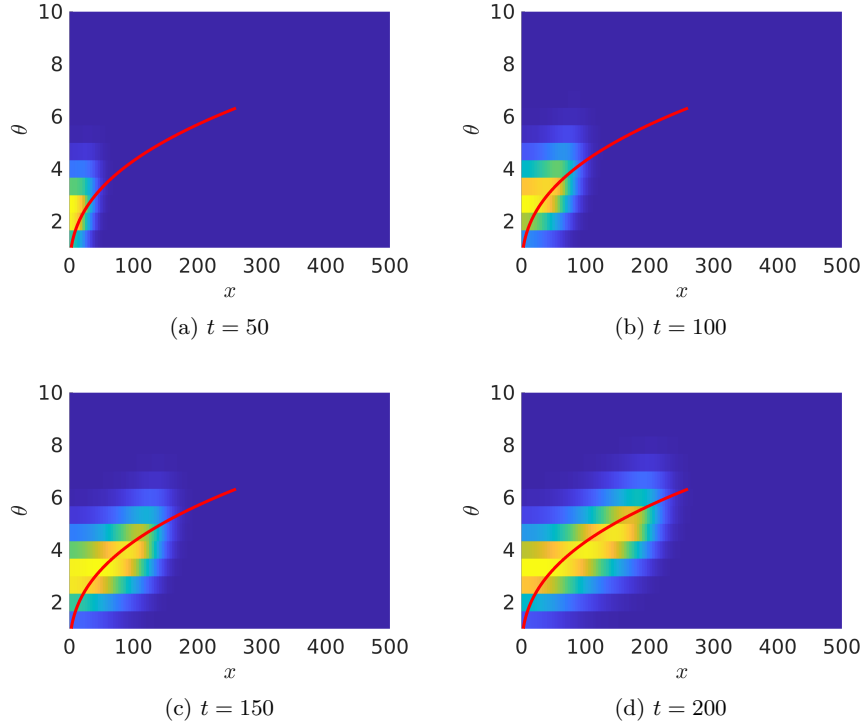


Figure 4: **Contour lines of the trait distribution during the invasion of a sexual population, initially gaussian distributed, with a different growth rate at low density** ($r = 0.1$), given by simulations, at (a) $t = 50$ (b) $t = 100$ (c) $t = 150$ (d) $t = 200$. The parameters are $\delta t = 0.02$, $\delta x = 4$, $\delta\theta = 2/3$, $x_{\max} = 3000$ and $\theta_{\max} = 201$. The red line represents the approximation of the mean trait behind the propagating front.

3 Simulations with a different value for λ

This last supplementary material is devoted to simulations of the invasion of a sexual population, initially gaussian distributed. We change the value of the segregational variance: we take $\lambda = 1$.

With these parameters, we have approximated the position of the propagating front at time $t \geq 0$ by:

$$X(t) = 4 \left(\frac{\lambda}{3} \right)^{1/2} r^{3/4} t^{5/4} = \frac{4}{\sqrt{3}} t^{5/4} \approx 2.31 t^{5/4}.$$

This seems again consistent with the simulations (see Fig. 5). This shows that when the segregational variance $\lambda^2 > 0$ is strong, the individuals can have individuals with better dispersive trait, which accelerate the invasion. In Fig. 6, we see that the approximation

given by the associated article is accurate.

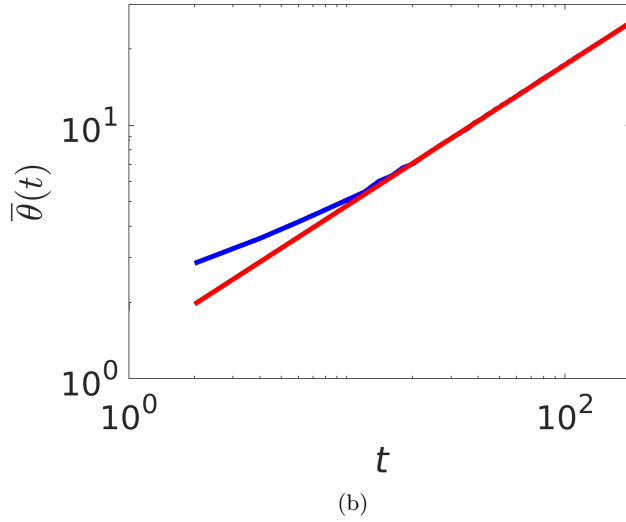
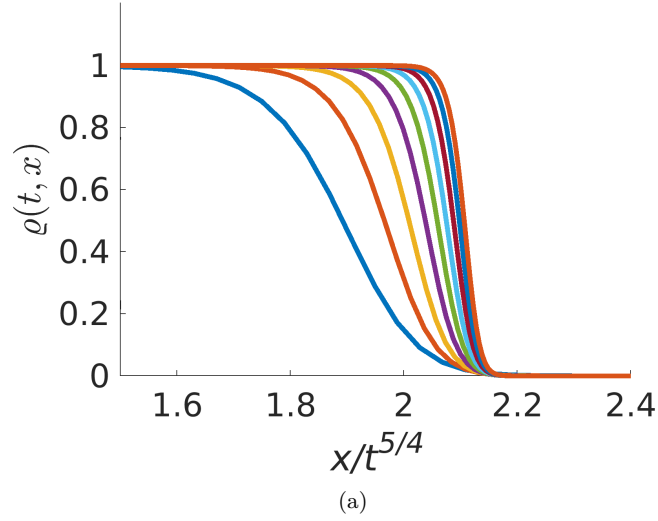


Figure 5: **Simulations of the invasion of a sexual population, initially gaussian distributed, with a different segregational variance** ($\lambda^2 = 1$), with parameters $\delta t = 0.02$, $\delta x = 4$, $\delta \theta = 2/3$, $x_{\max} = 3000$ and $\theta_{\max} = 201$. (a) Plot of the population size $\rho(t, \cdot)$ for successive fixed times at regular intervals from $t = 20$ to $t = 200$, with respect to the auto - similar variable $xt^{-5/4}$. (b) Plot of the mean of the dispersive trait $\bar{\theta}^{num}(t)$ at the front position with respect to time (blue curve) and of the function $t \rightarrow 1.34t^{0.56}$ (red curve), in log - log scale. The last funtion is given by a linear regression of the mean of the dispersive trait, with $R^2 = 1$.

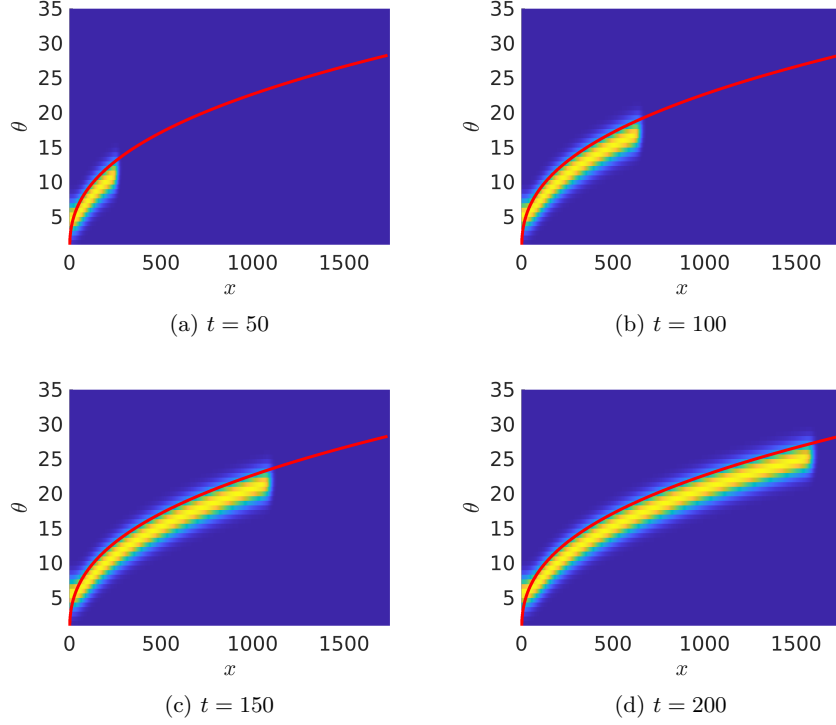


Figure 6: **Contour lines of the trait distribution during the invasion of a sexual population, initially gaussian distributed, with a different segregational variance ($\lambda^2 = 1$), given by simulations, at (a) $t = 50$ (b) $t = 100$ (c) $t = 150$ (d) $t = 200$.** The parameters are $\delta t = 0.02$, $\delta x = 4$, $\delta \theta = 2/3$, $x_{\max} = 3000$ and $\theta_{\max} = 201$. The red line represents the approximation of the mean trait behind the propagating front.